DERIVATION OF DIGITAL TERRAIN MODELS IN THE SCOP++ ENVIRONMENT

Norbert PFEIFER, Philipp STADLER and Christian BRIESE
Institute of Photogrammetry and Remote Sensing
Vienna University of Technology
np@ipf.tuwien.ac.at

KEY WORDS: DTM, laser scanning, filtering, classification, SCOP

ABSTRACT

Airborne laser scanning is widely used for the derivation of terrain information in wooded or open areas but also for the production of building models in cities. For this, the generation of a digital terrain model (DTM) is also required. In this paper the filtering and classification of laser scanner data with iterative robust linear prediction in a hierarchical fashion using data pyramids is described. The coarse-to-fine approach is advantageous because it strengthens the robustness of the method and makes it faster. The results for test data sets of the OEEPE are presented.

1 INTRODUCTION

Airborne laser scanning has become a widely used technique for the derivation of topographic data. The high degree of automation in both, capturing the data and processing the data, contributed to its fast spread. Currently, the main application for laser scanner data is the production of digital terrain models (DTM), whereas the fully automatic derivation of building models ((Wang and Schenk, 2000), (Morgan and Tempfli, 2000), (Brenner, 2000)) is not as operational yet. The automatic derivation of tree height and extraction of other forest stand parameters is investigated (Kraus and Rieger, 1999), as well as the automatic derivation of break lines in the laser data ((Brügelmann, 2000), (Wild and Krzystek, 1996)).

This paper will focus on the filtering of laser scanner data for obtaining elevation information in wooded as well as in built-up areas. The DTM is necessary for all the applications described in the previous paragraph. In the next section a short presentation of the algorithm developed at the Institute of Photogrammetry and Remote Sensing of the Vienna University of Technology (I.P.F.) will be given, especially the extension to the hierarchical approach will be treated. The following section will treat the user interface for the filtering program. The OEEPE test data are investigated in section 4. We are mainly concerned with the filtering and the accuracy determination.

2 ALGORITHM

The algorithm for filtering the laser scanner data was originally designed for laser data in wooded areas. Altering the values of some parameters and the application of a hierarchical approach made it possible to apply it also to city areas. In order to describe these extensions completely, a brief review of the algorithm will be given first. For a comprehensive description see (Kraus and Pfeifer, 1998) and (Pfeifer et al., 1999). Other filter algorithms based on mathematical morphology are described e.g. in (Vosselman, 2000), different approaches can be found in (Hansen and Vögtle, 1999) or (Axelsson, 2000). Unfortunately, the term *to filter* can have various meanings. On one hand it can mean the filtering (smoothing) of random measurement errors, on the other hand it stands for the filtering (elimination) of gross errors, which is also a classification. Unless stated otherwise we will always use the term in its second meaning.

In our algorithm — the iterative robust interpolation — a rough approximation of the surface is computed first. Next, the residuals, i.e. the oriented distances from the surface to the measured points, are computed. Each (z-)measurement is given a weight according to its distance value, which is the parameter of a *weight function*. The surface is then recomputed under the consideration of the weights. A point with a high weight will attract the surface, resulting in a small residual at this point, whereas a point that has been assigned a low weight will have little influence on the run of the surface. During these iterations a classification is preformed, too. If an oriented distance is above or below certain values, the point is classified as off–terrain point and eliminated completely from this surface interpolation. This process of weight iteration is perpetuated until all gross errors are eliminated (a stable situation) or a maximum number of iterations is reached.

There are two important entities in this algorithm. On one hand, the stochastic model, which is defined by the weight function, on the other hand, the functional model, which describes the way the surface is interpolated. Obviously, the

weight function must assign high values (close to 1) to ground points, which are below or on the averaging surface, and low values (weights close to 0) to the vegetation points which are above (or on) the averaging surface. The standard weight function of robust adjustment (used for example in bundle block triangulation) can be adapted to suit the needs for the interpolation and classification of laser scanner data. The function we use is not symmetrical, allowing a sharper decline for values above its origin (residuals belonging to vegetation points), and a slower decline — or no decline at all — for the ground point residuals. The graph of the weight function can be seen in fig. 1. Furthermore, the weight function does not need to be centered on the zero-point of the real axis. It can be shifted to the left (into the negative) for the interpolation of laser scanner data. What is more, the shift of the origin can be determined automatically, depending on the given data itself.

The interpolation method itself (functional model) is restricted to those methods which can consider the stochastic model described in the previous paragraph. This is possible for moving least squares ((Lancaster and Salkauskas, 1986)), kriging and linear prediction. These methods have in common that the surface is described as a sum of basis functions which are centered on the data points. However, the basis functions could also be arranged over a regular grid as e.g. in B–spline surface approximation (used for laser scanner data in (Kilian et al., 1996)). The basis functions themselves influence the rigidity of the surface. We use linear prediction which is very similar to kriging ((Kraus, 1998)). The covariance function (i.e. the basis function, corresponding to the variogram of kriging) is determined automatically, depending on the data itself.

What has been described so far is the core of the algorithm. Classification and DTM generation are performed in one step, there is no assumption that the terrain is horizontal. It is applied patch wise to the data, which results in an adaptive setting of the shift of the origin of the weight function. Furthermore, the basis functions are determined for each patch separately, too. However, in its present implementation the algorithm relies on a 'good mixture' of ground and off–terrain (vegetation) points, which can also be seen as a high frequency of change from ground to vegetation points. This is necessary for a reliable determination of the shift value for the origin of the weight function. What can be done if this high frequency is not given? One method is to extend the way the shift value is computed, the other is to provide the input data (points) in a suitable form. Because it is comparatively easy to establish these conditions (the suitable form) we chose to follow the second method, which will be explained in the following section.

Figure 1: User interface for the determination of the filter parameters. In the upper part the parameters of the weight function are defined, whereas the lower part is for the iteration control. Below the text 'Shift of origin of weight function', the user can decide whether to search for the shift value in the negative, the positive, or not at all. This can be done for the trend (plane) and the predicted surface.

2.1 Hierarchical approach

Our approach is comparable to a hierarchical setup using image pyramids, in our case data pyramids. The structure of these pyramids is regular (as in image processing) and typically two or three levels are sufficient. However, in comparison to image analysis, the reduction function operates on point data, not on pixels. (If the laser scanner data is provided as a digital geo-coded image where the grey values represent the terrain heights, the pyramids would indeed be image pyramids.) The method proceeds as follows:

1. Create the data sets with the lower resolutions,
2. filter the data and generate a DTM,
3. compare the DTM to the data of higher resolution and take points within a certain interval.

This process (steps 2 and 3) are repeated for each level, schematically it is shown in fig. 2 for two levels (level 0 and 1). Though this procedure can be applied to any data set of laser scanner data, or other data with gross errors, its advantages become important for dense data sets (0.5 point/m^2 or more). The method speeds up the filter process, enforces the elimination of houses and dense vegetation and makes the process more robust.

There are many possibilities to generate a coarser resolution (higher levels) of the given data (lower level, level 0 is the original data), the most straightforward techniques are to place a square grid (or any other tessellation) over the data and compute for each cell one point (regular pyramid). There are different methods to compute this point which are applicable for filtering of laser scanner data:

- Take the mean point in each cell.
- Take the lowest point in each cell.
- Take the point closest to the center in each cell.

Only the first of these reduction functions is linear (fast to compute), whereas the others are nonlinear. More complex methods can be performed by analyzing a histogram of the heights in each cell, but the methods described above are sufficient for our needs. Even more simple methods can be used. One possibility is to take every n-th point, which — under the pre-condition that the points have not been sorted after the measurement — maintains the ratios of point densities, though these data pyramids are not regular anymore. However, this method and the third method of the list, do not change the penetration rate of the data set. As the point density itself is diminished in this step we call it a *thin out*.

The second method speeds up the filtering, but there is the danger of taking a point which is a large (or small!) negative blunder. The third method provides a more regular structure of the generated point set. The choice of method can also be made depending on the kind of data (penetration rate, city or wooded area, ...). A thin out of the data has two advantages:

1. The regular structure of laser scanner data in built up areas (long sequences of points on the ground, on the roof, resp.) is broken apart.
2. The classification and filtering is accelerated, because a smaller data set is handled.

With the coarser data set a filtering is performed and a DTM is generated. Of course, embankments, break lines and other features are represented less distinctively than in the original data, but this is due to the coarser level of data, not due to the filtering. Therefore, for performing the filtering on the next lower level, the original point data (or the data of the corresponding pyramid level) and the DTM of the coarser level have to be combined to generate the data for the lower (finer) level. The original points and their distances to the DTM at the current resolution are analyzed. If they are within a certain interval they are accepted, otherwise they are rejected (sorted out). Thus, this step is called *sort out*. For laser scanner data the lower bound of this interval is negative (e.g. -1m) and the upper bound is positive (e.g. 1m). With this data set the next filter step can be performed. The choice of the intervals is not as critical as one might expect first, which is due to the filter step that is performed afterwards. Some vegetation points are included in the data set because they are relatively low to the ground, but they can be filtered in the next step.

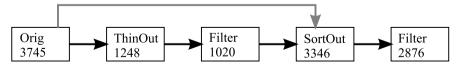| Orig 3745 | → | ThinOut 1248 | → | Filter 1020 | → | SortOut 3346 | → | Filter 2876 |

Figure 2: Schema of the hierarchical approach. The numbers below the names of the steps (taken from the Vaihingen data) represent: number of given points (Orig), reduced point number (ThinOut), ground points after filtering (Filter), number of points within a certain distance to the DTM (SortOut). The original data is used twice: first for the Thin Out, and later (after Filter, grey line) for the Sort Out.

3   LASER SCANNING WITHIN SCOP++

The algorithm described above is included in the program package SCOP (SCOP-WWW, 2001) for the derivation, application and presentation of DTMs. This set of programs is in use and applied in different environments (public authorities, universities, private companies). With the transition to SCOP++ (Dorffner et al., 1999) many new features have been introduced, amongst others:

- a graphical user interface (GUI) including project management,
- support for different data formats (Winput, DXF, ArcInfo, TIFF, JPEG, PDF, . . .),
- mixing of raster graphics (also of different resolutions and areas covered).

The extension for laser scanner data filtering will be available in the Extended Data Acquisition package of SCOP++. Fig. 3 shows the main window with the data of the eastern part of the Vaihingen example during an iteration step at the very beginning.

In the GUI-version of the laser data filtering, the user can, after project definition and data import, decide which strategy to use for the classification and filtering of the laser scanner measurements ('Strategy window'). These strategies distinguish themselves in the order of the particular steps ('thin out', application of filter algorithm, 'sort out') and the values for the parameters for these steps. However, the user can also create and apply a new strategy and save it for later re-use. Different
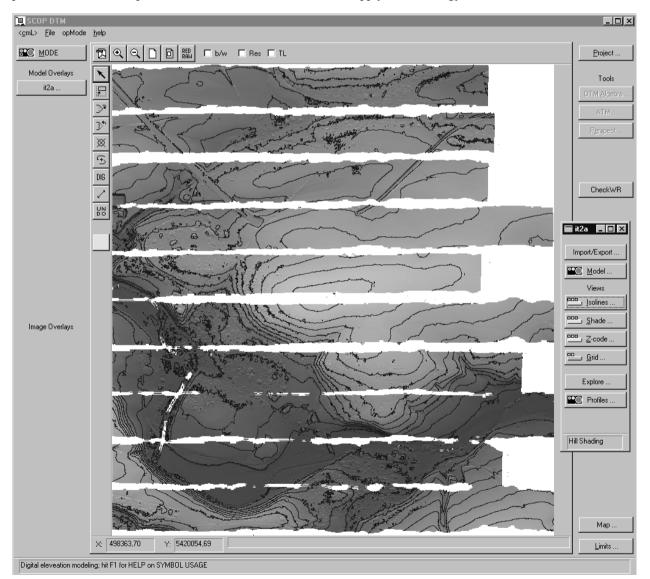

Figure 3: Main graphics window, showing a surface model in a combination of shading (from the north) and color coding (black to white) and the contour lines.

strategies are predefined for laser scanner data in city areas and wooded areas, but of course this list can be enlarged. As there is no perfect all-purpose filter algorithm, the purpose of the DTM could play a role here, too. Depending on the application, it may be worse to miss small dikes (e.g. flood simulation) whereas for other applications the correct representation of trenches may be more important.

In fig. 1 the window for the filter parameters is shown. In the upper middle is the graph of the weight function, to its left and right, are the settings for the negative and positive branch. Below the weight function the iteration control is situated. The first few numbers of iterations are normally performed with the trend (a tilted plane), which describes the surface sufficiently detailed, if the patches are small. Otherwise the number of iterations with the trend should be set to zero. The next iterations are performed with the predicted surface. For both kinds of iterations the shift of the origin of the weight function can be influenced. As mentioned above, it is set automatically, but the user can decide whether it should be searched in the negative, the positive, or not at all. A rough estimate of the penetration rate can be used to search for this shift value, too. The other parameters of the elevation model (accuracy of the points, size of patches, ...) can be defined under the 'Interpolation' button, which opens a window. The parameters in this window are necessary for all terrain models, not only for those derived with the iterative robust filtering.

4 OEEPE TEST

The Stuttgart data set and the Vaihingen data set provided by Fotonor have been used for the OEEPE laser scanning test. The data are in UTM32, based on the WGS84 co-ordinate system. First and last pulse and the intensities have been recorded simultaneously with an Optech laser scanner. The results for the TopoSys data set over Stuttgart (also available within the OEEPE test), captured with the TopoSys I laser scanner, are not included in this paper. Instead, the results of a vertical accuracy determination for this scanner in Vienna will be presented briefly.

The data sets have been processed with the hierarchical approach of the filter algorithm described above. Default values have been used for the parameters of the filter and no manual editing was performed. Tuning the parameters might have improved the result slightly but at the expense of more time spent. The processing of the data will be described in more detail for the Vaihingen data set, the filter results will be presented for both data sets. The vertical accuracy is determined with ground points for Vaihingen. For the Vaihingen and Stuttgart data sets small studies and preliminary results on the first–and–last pulse data and the intensities will be preseted.

4.1 Vaihingen

First, all strips were combined to one file. We used the Fotonor-'all'-data set, which contains the last recorded echo (pulse), because our aim was to filter the vegetation and houses and obtain a ground model. For practical reasons we split the data of the Vaihingen example in an eastern and a western part along the north-south line with easting 3495950m. Under our present working conditions (esp. computing environment) we process data sets of up to 4 mio. points as one unit. The eastern part will be treated in more detail. The size of this area is 25.27km^2. As it can be seen in the upper part of fig. 4 (a small part of the whole area, which can be seen in fig. 3) there are houses, vegetation and negative gross errors which have to be eliminated from the data set. The average point density is 0.23 points/m^2.

4.1.1 Data processing The relevant parameters for the filtering (including the hierarchical setup) can be found in tab. 1. The process is also shown in fig. 2. The first step is to thin out the data. As the data is sufficiently isotropically distributed every third point was taken to generate the coarser representation of the original point cloud. The minimum and maximum height in this area are 225.8m, 878.8m, respectively, but these elevations belong to gross error measurements.

The purpose of the second iteration (It.=2) is to eliminate negative blunders. Of course, also vegetation points above the terrain are eliminated during this step. After the first 5 iterations (maximum number of iterations at level 1, representing the first filter step in fig. 2), the 'sort out' is performed. The interval values of ±2m may seem very high, but the purpose

It.	surface	pts. 10^3	patch	tol+	tol–	HW+	HW–	pen.	off–terrain.
1	plane	1248	40x40m^2	3m	—	20cm	$-\infty$	50%	5.2%
2	plane	1184	15x15m^2	2.5m	–2.5m	20cm	$-\infty$	50%	2.9%
3-5	pred.	1149	45x45m^2	0.3m	–3m	20cm	$-\infty$	80%	11.2%
'sort out'		3745	—	2m	–2m				10.6%
6-8	pred.	3346	12x12m^2	0.1m	–0.3m	20cm	$-\infty$	85%	13.1%

Table 1: Parameters for the filtering of the Vaihingen example. The meaning of the columns is: number of iteration (It. 1–5 $\hat{=}$ level 1); type of computed surface (pred. $\hat{=}$ linear prediction); number of points on input; patch size; upper/lower bound for classification; positive/negative half-width value of weight function; penetration rate parameter; portion of points classified as off–terrain points.

of the previous iterations is mainly to eliminate the buildings and contiguous clusters of vegetation points without ground points in between. Additionally, these values ensure, that all points belonging to an embankment are in the new data set. In the following, a maximum number of 3 iteration steps (at level 0) are performed to eliminate the near ground vegetation and remaining building points.

In fig. 3 the elevation model after the second iteration (It.=2) is shown. A substantial part of the houses has already been eliminated. The wrinkles of the contour lines indicate, that the vegetation is not eliminated completely at this state. In fig. 4 a comparison between the original data and the filtered data after the last iteration step can be seen. Only a small part of the size of $0,82\text{km}^2$ of the complete eastern part of the Vaihingen data set is shown here. No manual intervention was performed during the iteration, the parameters used are default parameters and have not been adapted to this special data set, no manual deletion or inclusion of points was performed.

4.1.2 Result of Filtering The patches for the DTM computation were smaller for the original data. Thus, the void spaces in the upper half of the fig. 4 follow the strip more closely. The negative blunders have been eliminated completely. Also the houses are eliminated, but there remains a kind of ridge east of the middle. This appears to be a large but low building which could not be eliminated completely. The embankments have been preserved, though one of them (in the western part, running north-west in the lower strip) lost some of its sharpness. The vegetation has been eliminated completely. The remaining building could have been removed with a different set of parameters, but this would have eliminated more of the embankments.

The western part of this example has roughly the same dimensions as the eastern part and has been processed in exactly the same manner. The results are similar (see fig. 5). Negative blunders occurred in the western half as well, though none of them is shown in the figure.

As it can be seen, not all the houses have been eliminated completely. This is a consequence of the parameters and iteration settings, which are set for the removal of vegetation. A portion of the data holes have been closed, but of course,
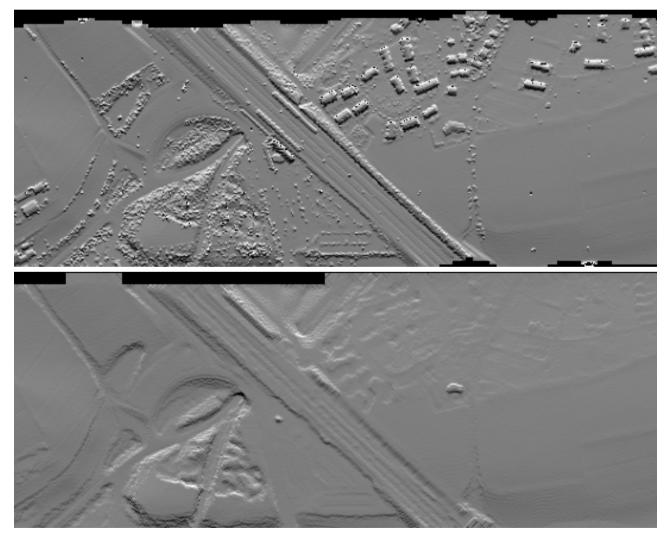

Figure 4: Vaihingen, original vs. filtered data in a shading, area: [(3496480, 5421370), (3497620, 5421806)]

the terrain height in these areas is questionable, although the terrain height is interpolated — more or less — linearly between the two sides. The diagonal pattern in the eastern part of the closed holes is a consequence of the (imperfect) interpolation (over point-less terrain) applied there.[1] In the selected area shown, north-west of the middle (at co-ordinates 3493791, 5419797), a structure can be seen which is presumably a natural, vegetated bump. It has been made smaller during the filtering, but equally it could have been a manmade structure. Again, the purpose the DTM is derived for, could solve the question whether to keep such structures or not. The setting of parameters will be affected by such a predetermination, too.

4.1.3 Accuracy determination For the area of Vaihingen the Institut for Photogrammetry at Stutgart University measured ground points with a Leica Wild GPS System 200 using a reference and a rover station. All together 4 areas with different terrain characteristics have been measured. Unfortunately, in 3 of these areas not all the points could be used, because of the lack of ground coverage from the laser scanner measurements. Furthermore, the Insitute for Photogrammetry observed a systematic vertical shift in the laser scanner data and determined it to be 0.35m. This shift was taken into account.

The vertical accuracies have been determined by means of an elevation model. The vertical distances from the check points to the elevation models were computed. For 3 of the 4 areas we used the terrain model derived as described in the previous subsections. However, as the filter algorithm could have eroded the railway ramps we computed an elevation model without filtering for this area. The vertical accuracies (under the assumption of error free check points) are shown

---

[1]For an easier interpretation of such artifacts we suggest the use of a quality layer (supplied with the DTM). It shows the reliability (average filter values, distance to nearest given point, ...) of the interpolation for a certain area.
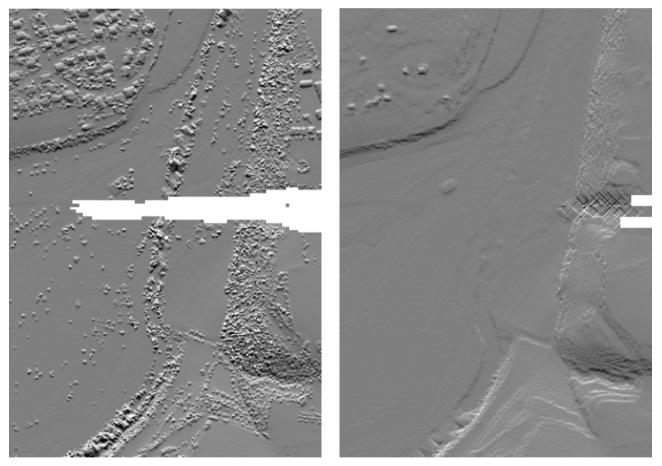

Figure 5: Original vs. filtered data in a shading, area: [(3493590, 5419300), (3494160, 5420120)], extension: 0.47km^2

area	r.m.s.	mean	max	point num.	characteristics
Grassland	0.11	+0.08	0.73	1368	different slope, smooth
Sport ground Vaihingen	0.08	+0.06	0.30	77	flat
Sport groung Illingen	0.08	+0.07	0.17	102	flat
Railway station	0.48	+0.39	1.46	210	railway ramp

Table 2: Accuracies for the test areas in Vaihingen. The last line has to be inspected carefully (see text). The unit for the accuracies is meter.

in table 2. For the first 3 areas there is still a systematic shift of about 7cm. This shows that the accuracy of a single laser measurement is even higher, but uncertainties in the determination of the transformation parameters and the modelling of the flight path and orientation will always remain. The area 'Grassland', which is not flat has a lower accuracy than the 2 flat sport grounds. This is an indication for a (systematic) horizontal shift. For the first 3 areas the r.m.s. error is 10.7cm. The errors for the railway ramp are higher. This is a consequence of the structure of the elevation model we used. As described above, we use a grid based model with a grid point distance of 1m, which is less than the point distance in the laser scanner data set. Because of the grid structure of the elevation model and because of the random point sampling of the laser scanner the edges are not represented correctly, break lines would be necessary for this. However, visual inspection of the co-ordinate values of the laser points and the check points showed, that the accuracies are similar to those of the other three examples. This means, that the accuracy of the laser scanner data for the railway ramp is better than what the table indicates on first sight.

4.1.4   First and last pulse data   The question arises, whether the first and last pulse data can be used to simplify or improve the filter process in wooded areas. Therefore, 6 rectangular areas of the Vaihingen data set were selected, all lying completely in wooded areas. The areas all together have an extension of $0.58km^2$. The characteristics can be seen in the left part of tab. 3. It is notable that the point density of 0.20 points/m^2 over the wooded areas is smaller than the average point density, which is 0.23 points/m^2.

First, the distances between the first and the last reflected pulse for each measurement were computed. When we speak of measurement we mean the position and intensity of the first and the last pulse (8 values). A histogram of the distribution of these distances can be seen in fig. 6, left side. For 19.7% the distances are smaller than 1m. These points are not necessarily ground points. It is also possible that the laser beam is reflected twice in the canopy or in medium layers of the trees. As it can be seen, the pulses are either very close to each other (within 1m), or more than 4m apart. The first–last distances go up to 40m, which also includes a few gross errors. The points were separated in two groups, the ones which are close to each other and the ones which have a higher distance (The threshold was 4m, but it could have been 1m as well, as it can be seen in the histogram.) These 2 groups have been compared to the ground model which was derived as described in section 4.1.1. For the time being, we assumed that the filtering worked 100% correct. Additionally, it can be assumed, that if the filtering is not completely correct, the errors occur only locally, for specific positions like peaks or steep descents. Thus, the errors — if any — induced by filtering errors are small in number.

The distances from the last pulse points to the ground model can be seen in the right part of fig. 6. The last pulse points range from 5m below the terrain to 36m above the terrain. For the measurements where the first and the last pulse are close to each other, 62.8% of the last pulse points lie within ±1m terrain distance, whereas for the points which have a

area				low distance				high distance			
	num.pt.	size	pt/m^2	num.	r.m.s.	mean	max	num.	r.m.s.	mean	max
1A	3135	0.015	0.207	617	6.97	3.89	25.67	2518	2.10	1.10	16.10
1B	12072	0.061	0.199	1058	4.35	1.26	32.70	11014	2.17	0.52	27.81
3	52152	0.251	0.208	12217	7.99	4.14	35.90	39935	3.02	0.93	30.76
4	12906	0.080	0.187	2468	8.14	3.97	30.83	12438	2.22	0.81	25.57
5	10601	0.049	0.214	2451	3.82	1.77	33.17	8150	2.58	0.87	26.85
10	25999	0.129	0.202	4676	4.77	1.75	28.92	21323	2.07	0.71	24.44
overall	118865	0.585	0.204	23487	6.95	3.26	—	95378	2.58	0.82	—

Table 3: Distances of last pulse points over wooded terrain. In the left part the number of points in each sample, the area size (km^2) and the density are shown. The middle part shows the distance to the terrain for those points, where the first and the last pulse are very similar. The same is shown for those points with large distances between first and last pulse in the right part. All the error measures (r.m.s., mean and max error) are in unit m.
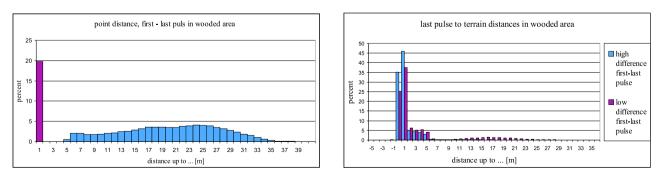

Figure 6: Laser scanner data over wooded terrain. *Left*: histogram of first–last pulse distances. *Right*: histogram of last pulse to terrain distances

higher difference between first and last pulse this number is 81.0%. Furthermore, 16% of the last pulse points lie between 10m and 30m above the terrain.

The penetration rate for this data set is about 77% (points within ±1m terrain distance). The chances that a last pulse point is a ground point are higher, if the distance between the first and the last pulse point is large, than if the distance is small. However, the differences are not too big. Furthermore, no strong correlation between the intensities over the forested areas and the distance from the last pulse to the filtered terrain could be proven. (The first intensity is usually low (dark), whereas the second is larger (bright).) The development and application of filter algorithms will stay important.

4.2   Stuttgart

As mentioned above, the Fotonor data set of Stuttgart is given in UTM32, based on WGS84. The point density for this data is higher than for Vaihingen, it is 0.81 points/m^2. The original data can be seen in the upper part of fig. 7.

4.2.1   Processing and Filtering the data   For Stuttgart, too, we used the Fotonor data set. Again the last pulse data was used in order to filter the vegetation and the houses. Again, because of the size of the test area, the data set was split
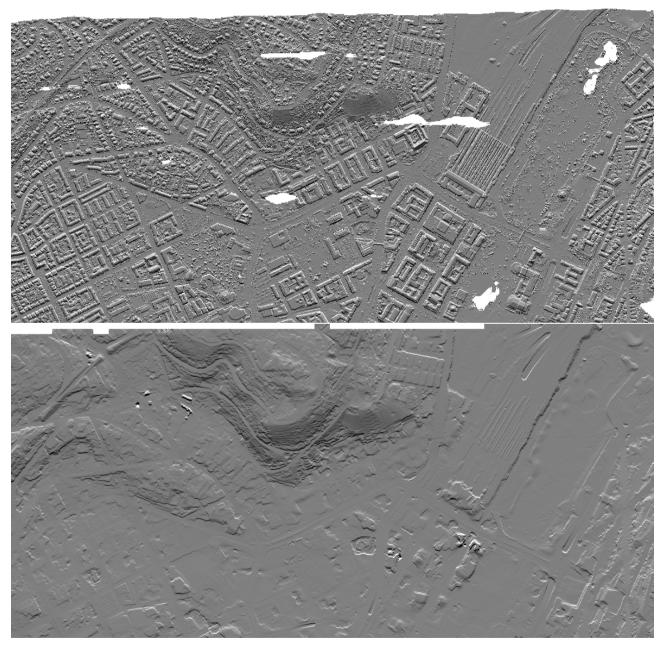

Figure 7: Northern part of Stuttgart, original data vs. ground model. A small number of buildings (e.g. the train station) were not eliminated.

into 2 parts at the east-west line with northing 5402900m. Thus, the norther part has an extension of 2500m by 1220m (3.05km^2, 2472834 points).

The processing of the data, the filtering of the houses and the vegetation, ran in the same way as the Vaihingen example, but the parameters were slightly different. First, the thin out was performed over a regular grid of 5m by 5m, choosing always the lowest point in each cell. While this speeded up the filtering, it also favored negative blunders. Apart from the patch sizes, which were slightly larger in this example, the parameters are the same as in tab. 1.

Fig. 7 shows the original data vs. the filtered data. Almost all houses were eliminated, only the biggest ones (the train station) remained. In the north-western part a few artifacts remained, also a big hole in the ground. This is, because we could not eliminate all negative blunders correctly in the automatic procedure. With minimal human intervention these errors were corrected.

4.2.2 First and last pulse and intensities

Like in Vaihingen, a histogram was computed which shows the distances between the first and the last pulse points. For 84.7% the distance is smaller than 25cm (fig. 8, left side). To record two distinctive echoes they must originate from surfaces which have a certain distance, which is at least half of the length of the wave package (pulse duration × speed of light). As it can be seen in the histogram the first and last pulse points are either more than 4m apart or identical.[2] There are point distances larger than 35m. To some extent these measurements may be due to high buildings which have been partially hit by the laser beam whilst the other part was reflected on the ground, but most of these measurements originate in gross errors. This is either a first pulse point which is much too high or a last pulse point which is below the terrain level. Both situations occur in the Stuttgart data set.

On the right hand side of fig. 8 the distribution of the intensity values of the first recorded pulse can be seen. The histogram for the second intensities looks similar, but with less entries below the intensity value 50 and more above this value. Furthermore, different methods have been performed to compute an ortho image with the recorded intensities which can be seen in fig. 9. The intensities from 0 to 250 have been assigned to the identical grey values, larger intensities were set to grey value 255. The images on the left hand side were generated using a 2 by 2m^2 raster. The intensities of all points falling in such a cell (which is determined with the x and y co-ordinate of the point) are averaged. The upper image shows this for the first intensities, the lower one for the last intensities. The choice of the cell size is critical. If it is too small, to many cells (pixels) obtain no value and the visual impression is unappealingly. In the upper left image 0.2% of the pixel represent no intensity value. If the cell size is too big, then image detail is lost. Therefore, the cell size has to be in the order of the average point distance. This problem can be avoided by interpolating a functional model (like an elevation model) with the intensity values as the observed function values and the x and y co-ordinates as the locations in the parameter domain (upper right image). This avoids the question of the cell size, only the grid size has to be chosen, which is much less critical. If it is too small, the processing time may increase, but no holes appear. For the upper right image a grid length of 1.5m has been chosen, thus the image is sharper. Here, also the first intensities were used.

The lower right image of fig. 9 shows a difference image of the first and last pulse image on the left side. The palette has been linearly scaled to cover the whole range. Single trees can be detected: in the first pulse data they appear black, in the last pulse data they have higher intensities.

---

[2]There is a small number of point pairs which is about 1 to 2m apart, preliminary inexplicable to us .
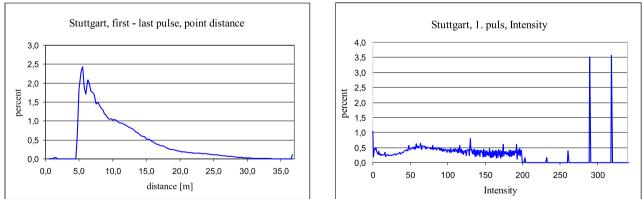

Figure 8: First and last pulse and intensity measurements of the Stuttgart data set (7,948,617 points). *Left*: Histogram of the distances between the first and last recorded echo for each emitted laser beam. For 85% the first and last pulse are identical (not shown in the histogram). *Right*: Distribution of the intensity values of the first pulse, 75% of the values are below 200, but the values go up to 5000 with gaps in between as on the right hand side.
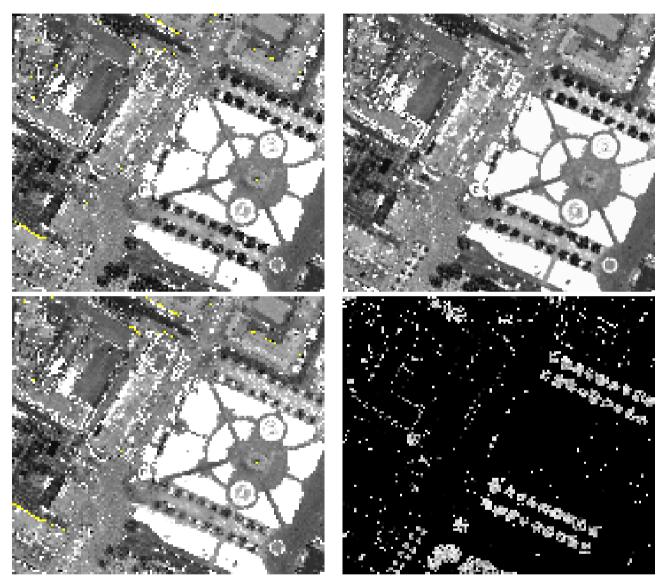
Figure 9: Ortho images from intensities. *Upper left*: regular 2 by 2m^2 grid, averaging of intensities in a cell, first intensties. *Lower left*: like upper image, second intensities. *Lower right*: difference image of first and second intensities, the histogram has been scaled. *Upper right*: image generated by interpolating intensities over a regular 1.5 by 1.5m^2 grid.

4.3 Vienna

For the City of Vienna our institute performed a laser scanner data examination with data of the TopoSys I scanner. The aim was to filter the vegetation and the houses and to determine the accuracy of the data. The test was carried out in 2000, initiated by the Vienna Municipal Department 41 – Surveyors. The test area had a size of $2.5km^2$. On the ground 816 check points were measured manually to determine the accuracy of the DTM (Briese et al., 2001). The results are shown in tab. 4. Partly the accuracies are better than the accuracy of a single laser measurement ($\pm$10cm), but for well defined, only slightly curved areas linear prediction produces an elevation model which is substantially more accurate than a single point measurement (Kraus, 2000). However, these accuracy values (r.m.s.) agree to those derived in section 4.1.3 for the Vaihingen data set.

description of region	r.m.s.	std.dev.
overall area	$\pm$10.5cm	$\pm$7.1cm
park, densed stock of trees	$\pm$14.5cm	$\pm$11.1cm
park, light stock of trees	$\pm$11.4cm	$\pm$7.8cm
park, open area	$\pm$8.6cm	$\pm$4.5cm
street, with parking cars	$\pm$9.2cm	$\pm$3.7cm
street, without cars	$\pm$2.4cm	$\pm$1.0cm

Table 4: Accuracies (r.m.s. of the residuals and standard deviation of the distribution of the residuals) of laser scanner derived DTM in a city.

5 CONCLUSIONS

In this paper we presented the iterative robust interpolation (using linear prediction) which has been embedded in a hierarchical approach. This improves the filter result and speeds up the computation. The software used is SCOP++, a GUI-version of the laser scanner extension will be available, too. With the OEEPE test data sets the suitability of the algorithm has been demonstrated.

The quality of laser scanner derived DTMs is very high. However, improvements can come from various sources. Especially the automatic detection of break lines in the laser data itself, or the utilization of extern data (e.g. digital maps) are important.

As the penetration rate can vary strongly in laser scanner data sets, a laser scanner DTM should be supplied together with a reliability and/or accuracy layer, indicating the quality of the model for a certain area. Furthermore, the purpose the DTM is used for plays a role during the filter process. For our algorithm this corresponds to different sets of parameters during the filter steps.

The simultaneous recording of first and last pulse and the intensities offers the possibility to obtain an ortho–image. The interpolation of the intensities is a suitable method to generate such images. Trees appear darker in a first intensities image and brighter in a last intensities image. For the area of Stuttgart we observed that 85% of the first and last pulses are identical (no difference in position), whereas for the wooded areas of the Vaihingen example this is only valid for 20%. Although more information is available with first and last pulse and intensity data, filtering still remains an important task.

Acknowledgements

REFERENCES

Axelsson, P. (2000). DEM generation from laser scanner data using adaptive tin models. In *International Archives of Photogrammetry and Remote Sensing, Vol. XXXIII, Part B4*, pages 111–118, Amsterdam, Netherlands.

Brenner, C. (2000). Towards fully automatic generation of city models. In *International Archives of Photogrammetry and Remote Sensing, Vol. XXXIII, Part B3*, pages 85–92, Amsterdam, Netherlands.

Briese, C., Kraus, K., Mandelburger, G., and Pfeifer, N. (2001). Einsatzmöglichkeiten der flugzeuggetragenen Laser-Scanner. In *Tagungsband der 11. Internationalen Geodätischen Woche in Obergurgl*. In print.

Brügelmann, R. (2000). Automatic breakline detection from airborne laser range data. In *International Archives of Photogrammetry and Remote Sensing, Vol. XXXIII, Part B3*, pages 109–115, Amsterdam, Netherlands.

Dorffner, L., Mandelburger, G., Molnar, L., Wintner, J., and Wöhrer, B. (1999). Geländemodelltechnologien - Forschung und Weiterentwicklung am I.P.F. In *Tagungsband der 10. Internationale Geodätische Woche in Obergurgl*, pages 31–44.

Hansen, W. and Vögtle, T. (1999). Extraktion der Geländeoberfläche aus flugzeuggetragenen Laserscanner–Aufnahmen. *Photogrammetrie Fernerkundung Geoinformation*, pages 229–236.

Kilian, J., Haala, N., and Englich, M. (1996). Capture and evaluation of airborne laser scanner data. In *International Archives of Photogrammetry and Remote Sensing, Vol. XXXI, Part B3*, pages 383–388, Vienna, Austria.

Kraus, K. (1998). Interpolation nach kleinsten Quadraten versus Krige-Schätzer. *Österreichische Zeitschrift für Vermessung & Geoinformation*, 1.

Kraus, K. (2000). *Photogrammetrie, Band 3, Topographische Informationssysteme*. Dümmler.

Kraus, K. and Pfeifer, N. (1998). Determination of terrain models in wooded areas with airborne laser scanner data. *ISPRS Journal of Photogrammetry and Remote Sensing*, 53:193–203.

Kraus, K. and Rieger, W. (1999). Processing of laser scanning data for wooded areas. In Fritsch and Spiller, editors, *Photogrammetric Week '99*, pages 221–231, Stuttgart, Germany. Wichmann Verlag.

Lancaster, P. and Salkauskas, K. (1986). *Curve and surface fitting, An Introduction*. Academic Press.

Morgan, M. and Tempfli, K. (2000). Automatic building extraction from airborne laser scanning data. In *International Archives of Photogrammetry and Remote Sensing, Vol. XXXIII, Part B3*, pages 616–623, Amsterdam, Netherlands.

Pfeifer, N., Köstli, A., and Kraus, K. (1999). Restitution of airborne laser scanner data in wooded area. *GIS Geo–Information–Systems*, 12:18–21.

SCOP-WWW (2001). http://www.ipf.tuwien.ac.at/produktinfo/scop/scop_dtm_sheet.htm. Institut of Photogrammetry and Remote Sensing, Vienna University of Technology.

Vosselman, G. (2000). Slope based filtering of laser altimetry data. In *International Archives of Photogrammetry and Remote Sensing, Vol. XXXIII, Part B3*, pages 935–942, Amsterdam, Netherlands.

Wang, Z. and Schenk, T. (2000). Building extraction and reconstruction from lidar data. In *International Archives of Photogrammetry and Remote Sensing, Vol. XXXIII, Part B4*, pages 958–964, Amsterdam, Netherlands.

Wild, D. and Krzystek, P. (1996). Automated breakline detection using an edge preserving filter. In *International Archives of Photogrammetry and Remote Sensing, Vol. XXXI, Part B3*, pages 946–952, Vienna, Austria.